NANO LETTERS

2004
Vol. 4, No. 2
317−321

Preferential Growth of Semiconducting Single-Walled Carbon Nanotubes by a Plasma Enhanced CVD Method

Yiming Li,[†,§] David Mann,[†,§] Marco Rolandi,[†,§] Woong Kim,[†] Ant Ural,[†] Steven Hung,[‡] Ali Javey,[†] Jien Cao,[†] Dunwei Wang,[†] Erhan Yenilmez,[†] Qian Wang,[†] James F. Gibbons,[‡] Yoshio Nishi,[‡] and Hongjie Dai*[,†]

Department of Chemistry and Laboratory for Advanced Materials, Stanford University, and Department of Electrical Engineering, Stanford University, Stanford, California 94305

Received November 28, 2003; Revised Manuscript Received January 8, 2004

ABSTRACT

Single-walled carbon nanotubes (SWNT) are grown by a plasma enhanced chemical vapor deposition (PECVD) method at 600 °C. The nanotubes are of high quality as characterized by microscopy, Raman spectroscopy, and electrical transport measurements. High performance field effect transistors are obtained with the PECVD nanotubes. Interestingly, electrical characterization reveals that nearly 90% of the nanotubes are semiconductors and thus highly preferential growth of semiconducting over metallic tubes in the PECVD process. Control experiments with other nanotube materials find that HiPco nanotubes consist of ∼61% semiconductors, while laser ablation preferentially grows metallic SWNTs (∼70%). The characterization method used here should also be applicable to assessing the degree of chemical separation of metallic and semiconducting nanotubes.

Single-walled carbon nanotubes (SWNTs) have been established as ballistic metallic and semiconducting molecular wires potentially useful for future high performance electronics.[1−4] To realize this potential, it is necessary to achieve preferential growth of semiconducting versus metallic nanotubes or enable high degrees of separation[5−8] of the two types of nanotubes. Here, we present synthesis of high quality SWNTs by a plasma enhanced CVD method at 600 °C, and an unexpected result that the PECVD method preferentially grows semiconducting nanotubes at a high percentage of ∼90%. The preferential growth has prompted us to investigate the percentages of semiconducting (s-SWNT) and metallic SWNTs (m-SWNT) in materials grown by other methods, both as control experiments and to elucidate these previously unknown parameters for some of the widely used nanotube materials. We conclude that the relative abundances of semiconducting and metallic nanotubes grown by various methods are different and do not necessarily follow the 2:1 ratio expected for random chirality distribution. Highly preferential growth of a certain type of SWNT can occur depending on the growth method. The results and characterization method presented here should also have implications to chemical separation of nanotubes.

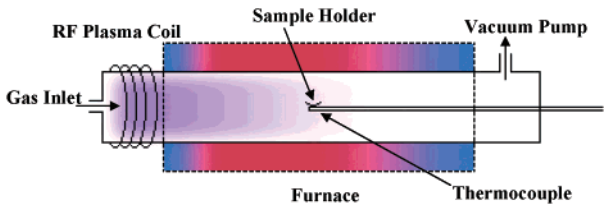

Figure 1. Schematic drawing of the PECVD reactor used for the synthesis of SWNTs.

A home-built radio frequency (RF, 13.56 MHz) 4-in. remote PECVD system[9] was used for nanotube growth (Figure 1). The plasma discharge source consisted of a copper coil wound around the outside of the 4-in. quartz tube near the feed-gas entrance. We operated the plasma in capacitive mode with the interior furnace wall acting as an electrode and the coil acting as the counter electrode. This created a low-density plasma that propagated down the interior of the quartz tube and reached the sample placed at the center of the tube reactor, 40 cm away from the plasma coil. The

* Corresponding author: hdai@stanford.edu.
† Department of Chemistry and Laboratory for Advanced Materials.
‡ Department of Electrical Engineering.
§ These authors contributed equally.

10.1021/nl035097c CCC: $27.50
Published on Web 01/22/2004

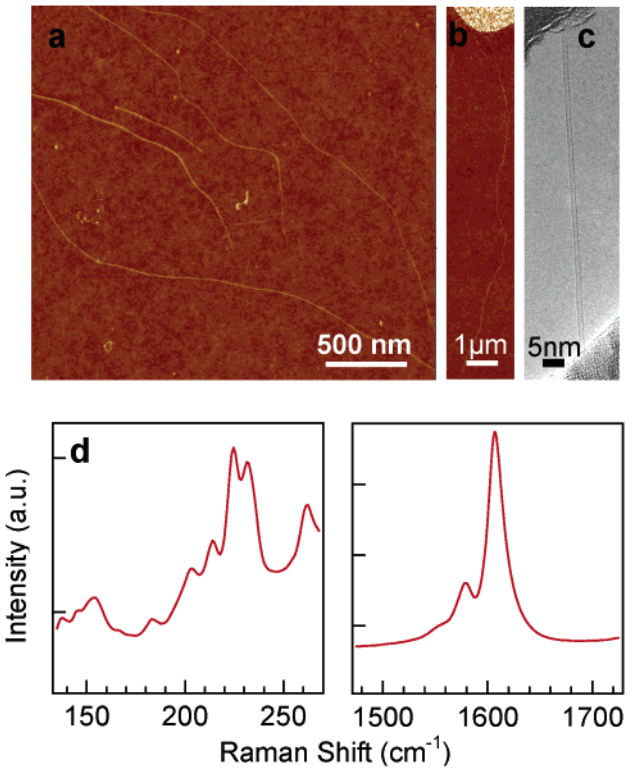

Figure 2. SWNTs grown at 600 °C. (a) AFM image of nanotubes grown from low-density ferritin deposition on a SiO_2 substrate. (b) AFM image of a tube grown from an iron-film island (nominal thickness 1 Å). (c) TEM image of an as-grown SWNT (diameter = 1.2 nm). (d) Left panel: Raman data for the RBMs of SWNTs grown by PECVD. Right panel: The G-band of SWNT vibration (clear peaks at 1578 and 1608 cm^{-1}, due to splitting of the in-plane graphene mode at 1580 cm^{-1} from graphene to tubes). Raman data here was obtained with a SWNT mat grown on a uniform Fe film deposited on SiO_2, and the data were sum of 75 spectra recorded over the sample.

sample underwent no local heating due to the plasma, as verified by a thermocouple located directly under the sampleholder. The design of the PECVD system is such that the plasma can be operated in inductively coupled mode as well, though the transition from capacitive to inductive mode occurs at far higher input power than is used for the current work.

Nanotube growth was carried out on SiO_2/Si wafers (SiO_2 thickness $t_{ox} = 67$ nm) or on holey-SiO_2 films supported on transmission electron microscope (TEM) grids. Two types of catalysts were used in this work. The first was discrete ferritin particles with an average of ~300 Fe atoms per ferritin,[10] adsorbed randomly onto the SiO_2/Si substrates or onto the SiO_2 TEM grids from a solution. The density of the ferritin particles, controlled by the ferritin concentration and the adsorption time, was less than one monolayer. The second type of catalyst was nominally ~1 Å thick Fe films formed by slow electron beam evaporation at a rate of 0.1 Å for 3−12 s monitored by a quartz crystal microbalance. SiO_2/Si substrates with patterned catalyst islands[11] of ~1 Å Fe films were also used for growth. The catalyst-deposited substrates were heated to 600 °C in Ar, after which methane (80% CH_4 in Ar) was introduced into the reactor at a flow rate of ~60 sccm (standard cubic centimeter per minute) under vacuum pumping to reach a pressure of ~500 mTorr. The plasma source was then turned on (RF power ~75 W) for 3 min for PECVD growth. The plasma and CH_4 were then switched off and the system was cooled to room temperature in Ar.

Atomic force microscopy (AFM) revealed that nanotube-like structures grew from ferritin and thin Fe film catalysts (Figure 2a,b). Topographic height measurements revealed tube diameters of $d = 0.8$ nm to 1.5 nm with a mean of ~1.2 nm. TEM provided direct evidence that the nanotubes grown directly on the grids were single-walled (Figure 2c) and free of obvious kinks or other types structural defects. Furthermore, resonant Raman spectroscopy[12,13] data, recorded with a Renishaw 1000 micro-Raman spectrometer with a laser excitation of $\lambda = 785$ nm, clearly resolved the radial breathing modes (RBM) and the G-band of the SWNTs (Figure 2d) grown from a thin Fe film on a SiO_2/Si substrate. Raman data confirmed the diameter distribution of $d = 0.8-1.5$ nm for the PECVD tubes according to[13] $\omega_{RBM}(cm^{-1}) = 12.5 + 223.5/d(nm)$, where ω_{RBM} is the Raman shift for the RBM.

Transport measurements of the PECVD SWNTs were performed to elucidate the electrical properties and test the quality of the nanotubes. Substrates with nanotubes grown from ferritin particles with various densities were used for device fabrication. We randomly fabricated an array of source/drain (S/D) electrode pairs on such a substrate, and then used AFM and electrical probing to identify the devices with nanotubes bridging the S/D. In control experiments, HiPco or laser ablation materials were sonicated in chloroform for 15 min, to afford mostly individual nanotubes, and deposited onto substrates by spin casting. Electrical devices were then obtained similar to the case for PECVD nanotubes. Pd was used for S/D electrodes[2,14] in the top-contact geometry, and the gap between the S/D electrodes was small ($L \sim 300$ nm) for all of our devices.

We found that at the high end of the diameter range, PECVD s-SWNTs with $d \sim 1.5$ nm exhibited ON-conductance of $G_{on} = 0.06G_0 = 0.06 \times 4\ e^2/h$ (resistance $R_{on} \sim 100$ kΩ) and an on- and off-current ratio of $I_{on}/I_{off} = 10^6$ (Figure 3a) with I_{on} near 10 μA (Figure 3b). Two of the performance parameters, G_{on} and I_{on}, were at least comparable to s-SWNTs with $d \sim 1.5$ nm grown by regular CVD and laser ablation. However, since the majority of the PECVD SWNTs were small, $d \sim 1$ nm, the devices typically exhibited low $G_{on} \sim 0.001G_0$ and $I_{on} \sim 1$ μA. Very similar properties were measured for HiPco tubes with $d \sim 1$ nm. These electrical characteristics do not necessarily imply low quality of either the PECVD or the HiPco material. Small diameter SWNTs have band gaps near 1 eV and the formation of highly transparent contacts to these tubes were difficult even with the high work function metal Pd.[2] The existence of Schottky barriers[2,15] at the contacts could be mainly responsible for the low conductance.

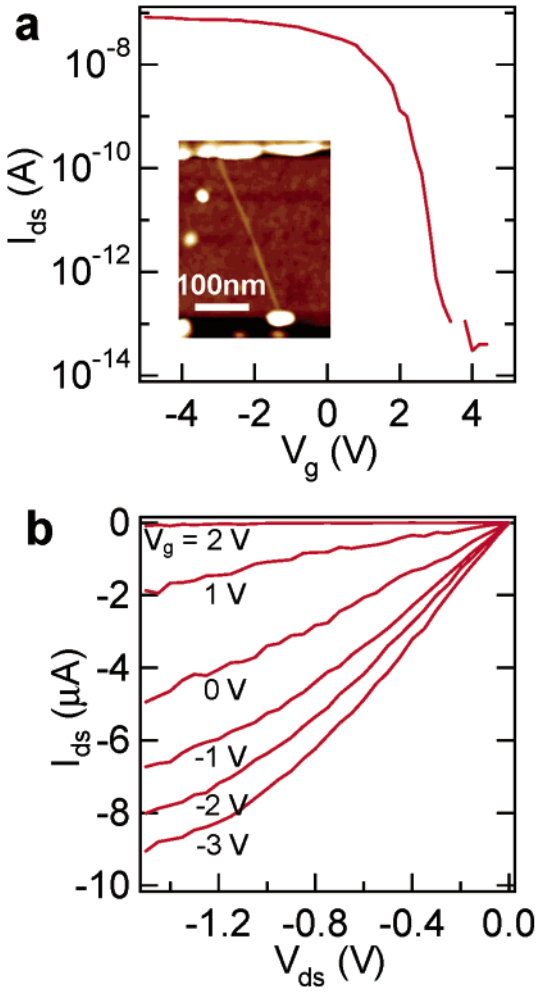

Figure 3. A transistor based on a PECVD SWNT. (a) Current (I_{ds}) vs gate voltage (V_g) for a single-tube device recorded under a bias of $V_{ds} = 10$ mV. The inset shows an AFM image of the device (SWNT $d \approx 1.5$ nm, channel length $L \sim 300$ nm). The on-state resistance is $R = 100$ kΩ under $V_g = -5$ V. (b) Current vs bias under various V_g for the device showing a high on-current near 10 μA. Note that this particular device was passivated with a poly(methyl methacrylate) layer to eliminate hysteresis caused by adsorbed water molecules.[24]

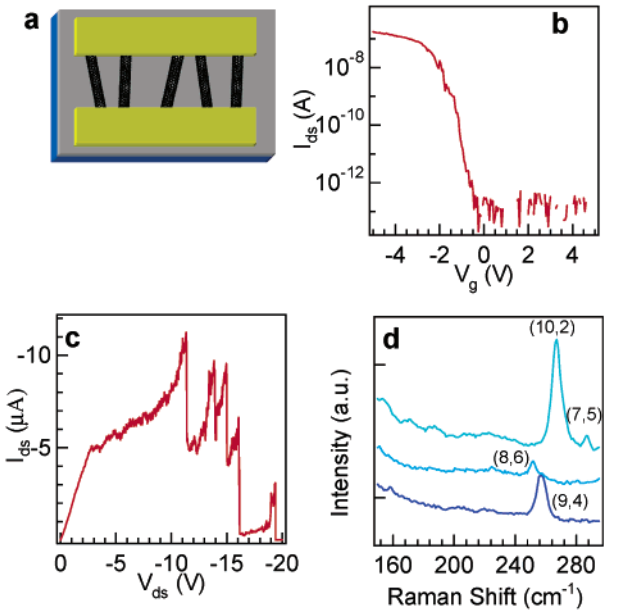

Figure 4. A 5-tube-in-parallel transistor derived by PECVD. (a) Schematic drawing of the device. (b) I_{ds} vs V_g for the five-tube device showing conductance depletion ($I_{on}/I_{off} = 10^5$, $V_{ds} = 100$ mV). (c) I_{ds} vs V_{ds} showing sequential electrical breakdown of the tubes in the device. (d) RBM micro-Raman data of the area between the S/D electrodes identifies four semiconductor SWNTs in resonance with the laser. The peaks were labeled with structural (m,n) indices (all corresponding to s-SWNTs) using earlier methods.[12,13]

In the initial stages of this work, we noticed unusually high percentages of devices fabricated with as-grown PECVD SWNTs behaving like semiconductor FETs with complete conductance depletion under electrostatic gating ("depletion" or "depletable" hereafter is defined for devices with $I_{on}/I_{off} > 10^4$). This prompted us to perform a systematic investigation with six batches of samples (with a total of ~ 20 chips) to quantify the percentage of s-SWNTs grown by PECVD. One method of quantification is to use AFM to identify electrically connected devices with individual SWNTs bridging the electrodes, and then determine if the nanotubes exhibit semiconducting or metallic characteristics by electrical measurement. With one batch of sample, we obtained about 30 single-tube devices out of 98 on each chip. With a total of four chips, we measured $N_T = 138$ individual nanotube devices and found that the number of s-SWNTs is $N_s = 124$, corresponding to a high percentage of $p = 89.8\%$. The error bar for the statistics is determined by the number of tubes investigated and is $\sim 1.96 \times [p(1-p)/N_T]^{1/2} = 5.0\%$ for a confidence coefficient of 95%.[16] Note that it is critical to survey large numbers of nanotubes in order to avoid large errors in the statistics. For an example, if a percentage of p ~ 67% was obtained based on only $N_T = 30$ tubes, then the error bar would be ~17%, making the statistics very imprecise.

Identifying individual nanotubes in large arrays of devices by AFM imaging is laborious. A second method that we used to quantify s- vs m-SWNTs was based on devices consisting of multiple (~1−7) SWNTs bridging wide (~10 μm) S/D electrodes. Note that for a given areal density of nanotubes on a substrate, the width of the S/D electrodes can be varied (5−15 μm) to obtain approximate control over the average number of SWNTs bridging the S/D in each device. The numbers of m- and s-SWNTs in each device were measured by using electrical breakdown of SWNTs[17] and counting the number of abrupt current drops under increased S/D bias voltage. For a depletable device, we applied a high negative gate voltage ($V_g = -5$ V) to ensure all s-SWNTs bridging the gap were in the "on" state, and increased the bias voltage until the current dropped to zero. Figure 4c shows a depletable device exhibiting five abrupt current drops. For a nondepletable device (defined as $I_{on}/I_{off} < 10^4$), we first cut ($V_g = +10$ V under which s-SWNTs were off) and counted the number of m-SWNTs until the device became depletable, and then cut and counted s-SWNTs (under $V_g = -5$ V). Figure 5 shows that a 7-tube nondepletable device became depletable (Figure 5a) after cutting one m-SWNT (Figure 5b inset). Continued cutting of the now depletable

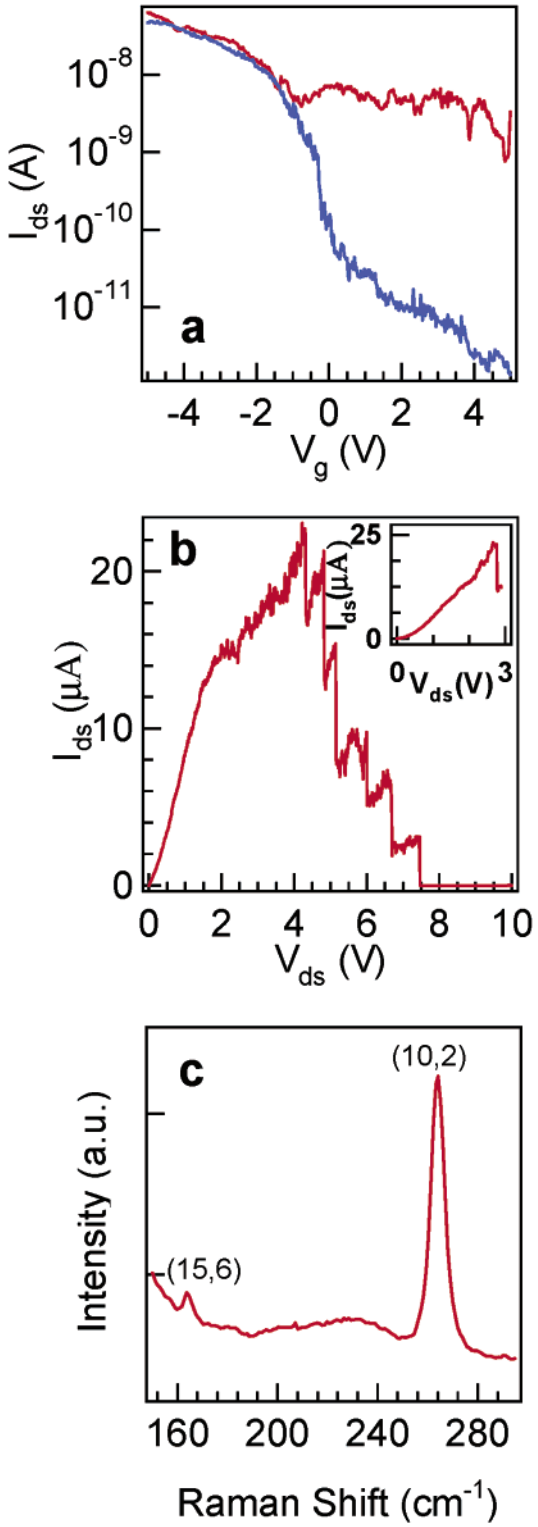

Figure 5. Counting of metallic and semiconducting SWNTs. (a) I_{ds} vs V_g (under $V_{ds} = 100$ mV) data for a seven-tube device before (higher curve) and after (lower curve) cutting one m-SWNT. (b) Inset shows cutting of one m-SWNT, after which the lower curve in (a) was recorded. The main panel shows continued cutting of six s-SWNTs in the device. (c) Micro-Raman data reveal one (15,6) m-SWNT and one (10,2) s-SWNT resonating with the 785 nm laser in this device.

device revealed 6 s-SWNTs (Figure 5b). This cutting and counting method was very efficient since AFM imaging of large numbers of devices was not needed. We did carry out AFM on some of the devices and found that the number of nanotubes revealed by AFM matched that found by the cutting method, which suggests that simultaneous breakdown of multiple nanotubes during cutting is very rare. With a particular batch of 157 devices, the cutting and counting method identified 89.5% s-SWNTs out of a total of $N_T = 439$ tubes.

We also used resonance micro-Raman[12] spectroscopy to acquire the spectroscopic signatures of PECVD SWNTs in devices that had been characterized by electrical measurements. For multitube depletable devices, Raman spectroscopy consistently revealed s-SWNTs with identifiable chiral (m,n) indices[12,13] (Figure 4d) and never encountered m-SWNTs in the devices. Raman measurements of multitube nondepletable devices were able to occasionally identify m-SWNTs (Figure 5c), but the occurrence of m-SWNTs was much less frequent than s-SWNTs. Note that micro-Raman spectroscopy (similar experimental setup and procedure as in ref 13) was used here to provide a local spectroscopic sampling of tubes in our devices. It was by no means intended to characterize the relative abundance of m- and s-SWNTs and identify every tube in the devices, since the 785 nm laser excitation only resonates with a fraction of SWNTs.

Out of a total of $N_T = 701$ nanotubes characterized by the two electrical characterization methods combined, we found a percentage of 89.3 ± 2.3% s-SWNTs grown by PECVD (Table 1). This unusually high percentage strongly suggests preferential growth of semiconducting SWNTs in our CVD process. In control experiments, we investigated as-grown HiPco[18] and laser ablation[19] SWNTs using the electrical cutting method described above. We found ~61.0 ± 7.6% and ~30.0 ± 6.0% s-SWNTs for HiPco (Table 1) and laser ablation (W. Kim and H. Dai, unpublished data) materials, respectively. Noteworthy is that these percentages were unknown in the literature despite the wide use of these nanotube materials. Interestingly, the percentage of semiconductors in HiPco samples falls within the margin of error for materials with no chirality preference (similar to SWNTs grown by regular CVD[11,20]), while laser ablation preferentially produces metallic SWNTs (~70%).

Our current work was initially aimed at lowering the growth temperature for SWNTs from ~800−900 °C typically involved in CVD.[11,20] Lower temperature should significantly enhance the compatibility of nanotube synthesis with CMOS technology for hybrid electronics. Also, the size and shape of catalytic nanoparticles should be more stable at lower temperatures, which should facilitate better control over the size and potential chirality of nanotubes. With PECVD, we were indeed able to significantly lower the growth temperature for SWNTs. The plasma-assisted dissociation of CH_4 into more reactive higher hydrocarbons and more reactive radicals must be responsible for efficient SWNT growth at 600 °C. No nanotubes were grown without the plasma assistance under otherwise identical conditions. Note that a low temperature growth method for SWNTs was reported recently by CVD of alcohol.[21] After

Table 1. Summary of the Diameter Distributions and Percentages of s- and m-SWNTs Grown by PECVD (with several batches of devices) and HiPco

	measured Raman RBM (cm^{-1})	diameter range (from Raman)	total # of devices	total # of Tubes (N_T)	# of s-SWNTs (N_s)	# of m-SWNTs	s-SWNT % = (p)
PECVD	161−284	0.8 nm−1.5 nm	375	701	626	75	89.3 ± 2.3%
HiPco	201−264	0.8 nm−1.3 nm	80	164	100	64	61.0 ± 7.6%

this work was finished, we learned about a PECVD work for SWNT synthesis, though they presented no characterization of their SWNTs beyond TEM and Raman spectroscopy.[22]

Unfortunately, an understanding of the mechanism for the preferential growth of semiconducting SWNTs in the PECVD process is lacking at the present time. Various parameters and factors involved in the PECVD process could be responsible for the preferential growth of semiconducting nanotubes. Compared to regular methane CVD that produces nanotubes without preference to s- or m-SWNTs, the current growth process is clearly different in lower growth temperature and the involvement of plasma. The roles played by these factors in preferential growth of s-SWNTs remain to be determined and merit further investigation. Although we cannot yet elucidate whether temperature, presence of plasma, or other factors unrecognized underlie the preferential growth phenomenon, we can conclude that preferential formation of certain types of nanotubes does occur for s-SWNTs in the PECVD process and for m-SWNTs in laser ablation. Also noteworthy is that it was reported recently that for s-SWNTs, certain chirality nanotubes are favored to grow under specific CVD growth conditions.[23]

Finally, we suggest that our results may have implications to chemical separation of carbon nanotubes, an approach that has made substantial progress recently.[5−8] Quantification of semiconducting and metallic nanotubes in the starting material and in the separated fractions is key to assessing the degree of separation, but has not been made thus far. The elegant spectroscopy characterization techniques have provided information about the relative abundance of metallic or semiconducting nanotubes, but not the quantitative percentages of metallic and semiconducting nanotubes. Spectroscopy analysis combined with electrical characterization methods such as the ones shown here (or scanning tunneling microscopy measurements) could provide the ultimate evidence of successful separation of nanotubes.

Acknowledgment. This work was supported by the Stanford Initiative for Nanoscale Materials and Processes (INMP) and DARPA/Moletronics.

References

(1) Javey, A.; Kim, H.; Brink, M.; Wang, Q.; Ural, A.; Guo, J.; McIntyre, P.; McEuen, P.; Lundstrom, M.; Dai, H. *Nature Materials* **2002**, *1*, 241.
(2) Javey, A.; Guo, J.; Wang, Q.; Lundstrom, M.; Dai, H. J. *Nature* **2003**, *424*, 654.
(3) McEuen, P. L.; Fuhrer, M. S.; Park, H. K. *IEEE Trans. Nanotechnol.* **2003**, *1*, 78.
(4) Wind, S.; Appenzeller, J.; Martel, R.; Derycke, V.; P, P. A. *Appl. Phys. Lett.* **2002**, *80*, 3817−3819.
(5) Chattopadhyay, D.; Galeska, L.; Papadimitrakopoulos, F. *J. Am. Chem. Soc.* **2003**, *125*, 3370.
(6) Krupke, R.; Hennrich, F.; vonLohneysen, H.; Kappes, M. M. *Science* **2003**, *301*, 344.
(7) Zheng, M.; Jagota, A.; Semke, E. D.; Diner, B. A.; Mclean, R. S.; Lustig, S. R.; Richardson, R. E.; Tassi, N. G. *Nature Materials* **2003**, *2*, 338.
(8) Chen, Z.; Du, X.; Du, M.-H.; Rancken, C. D.; Cheng, H.-P.; Rinzler, A. G. *Nano Lett.* **2003**, *3*, 1245−1249.
(9) Hung, S. Ph.D Thesis; Stanford University, 2003.
(10) Li, Y.; Kim, W.; Zhang, Y.; Rolandi, M.; Wang, D.; Dai, H. *J. Phys. Chem. B* **2001**, *105*, 11424.
(11) Kong, J.; Soh, H.; Cassell, A.; Quate, C. F.; Dai, H. *Nature* **1998**, *395*, 878.
(12) Jorio, A.; Saito, R.; Hafner, J. H.; Lieber, C. M.; Hunter, M.; McClure, T.; Dresselhaus, G.; Dresselhaus, M. S. *Phys. Rev. Lett.* **2001**, *86*, 1118−1121.
(13) Bachilo, S. M.; Strano, M. S.; Kittrell, C.; Hauge, R. H.; Smalley, R. E.; Weisman, R. B. *Science* **2002**, *298*, 2361−2236.
(14) Mann, D.; Javey, A.; Kong, J.; Wang, Q.; Dai, H. *Nano Lett.* **2003**, *3*, 1541.
(15) Heinze, S.; Tersoff, J.; Martel, R.; Derycke, V.; Appenzeller, J.; Avouris, Ph. *Phys. Rev. Lett.* **2002**, *89*, 6801.
(16) Mendenhall, W.; Beaver, R. J.; Beaver, B. M. *Introduction to probability and statistics*, 11th ed.; Brooks/Cole-Thomson Learning: Pacific Grove, CA, 2003.
(17) Collins, P. C.; Arnold, M. S.; Avouris, Ph. *Science* **2001**, *292*, 706.
(18) Nikolaev, P.; Bronikowski, M. J.; Bradley, R. K.; Rohmund, F.; Colbert, D. T.; Smith, K. A.; Smalley, R. E. *Chem. Phys. Lett.* **1999**, *313*, 91−97.
(19) Thess, A.; Lee, R.; Nikolaev, P.; Dai, H. J.; Petit, P.; Robert, J.; Xu, C. H.; Lee, Y. H.; Kim, S. G.; Rinzler, A. G.; Colbert, D. T.; Scuseria, G. E.; Tomanek, D.; Fischer, J. E.; Smalley, R. E. *Science* **1996**, *273*, 483−487.
(20) Kim, W.; Choi, H. C.; Shim, M.; Li, Y.; Wang, D.; Dai, H. *Nano Lett.* **2002**, *2*, 703.
(21) Maruyama, S.; Kojima, R.; Miyauchi, Y.; Chiashi, S.; Kohno, M. *Chem. Phys. Lett.* **2002**, *360*, 229.
(22) Kato, T. et al. *Chem. Phys. Lett.* **2003**, *381*, 422.
(23) Bachilo, S. M.; Balzano, L.; Herrera, J. E.; Pompeo, F.; Resasco, D. E.; Weisman, R. B. *J. Am. Chem. Soc.* **2003**, *125*, 11186.
(24) Kim, W.; Javey, A.; Vermesh, O.; Wang, Q.; Li, Y.; Dai, H. *Nano Lett.* **2003**, *3*, 193.

NL035097C